HHS Public Access

Author manuscript

J Immunol. Author manuscript; available in PMC 2017 September 15.

Published in final edited form as:

J Immunol. 2016 September 15; 197(6): 2316–2324. doi:10.4049/jimmunol.1600544.

B cell responses associated with vaccine-induced delayed SIV_{mac251} acquisition in female rhesus macaques

Venkatramanan Mohanram[*], **Thorsten Demberg**[*], **Thomas Musich**[*], **Iskra Tuero**[*], **Diego A. Vargas-Inchaustegui**[*], **Leia Miller-Novak**[*], **David Venzon**[†], and **Marjorie Robert-Guroff**[*,‡]

[*]Section on Immune Biology of Retroviral Infection, Vaccine Branch, NCI, NIH, Bethesda, MD 20892

[†]Biostatistics and Data Management Section, National Cancer Institute, Bethesda, MD 20892, USA

Abstract

An established sex bias in HIV pathogenesis is linked to immune responses. Recently we reported a vaccine-induced sex bias: vaccinated female but not male rhesus macaques exhibited delayed SIV acquisition. This outcome was correlated with SIV Env-specific rectal IgA, rectal memory B cells, and total rectal plasma cells (PC). To uncover additional contributing factors, using samples from the same study we investigated memory B cell population dynamics in blood, bone marrow (BM) and rectal tissue during immunization and post-challenge; IgG subtypes and antibody avidity; and B_{reg} cell frequency and function. Few sex differences were seen in Env-specific memory B cell, plasmablast or PC frequencies in the three compartments. Males had higher IgG antibody titers and avidity indices than females. However, females had elevated levels of Env-specific IgG1, IgG2, and IgG3 antibodies compared to males. gp140-specific IgG3 antibodies of females but not males were correlated with ADCC activity against gp120 targets ($p = 0.026$) and with antibody-dependent phagocytic activity ($p = 0.010$). IgG3 antibody of females but not males also correlated with decreased peak viremia ($p = 0.028$). Peripheral blood $CD19^+CD25^+$ B_{reg} cells suppressed T cell proliferation compared to $CD19^+CD25^-$ cells ($p=0.031$), and exhibited increased IL-10 mRNA expression ($p=0.031$). Male macaques post-vaccination ($p=0.018$) and post-infection ($p=0.0048$) exhibited higher B_{reg} frequencies than females. Moreover, male B_{reg} frequencies correlated with peak viremia ($p=0.0071$). Our data suggest that vaccinated females developed better antibody quality, contributing to better functionality. The elevated B_{reg} frequencies in males may have facilitated SIV acquisition.

INTRODUCTION

Human immunodeficiency virus (HIV), the causative agent of AIDS, has claimed an estimated 1.2 million lives and was responsible for 2 million new infections globally in 2014 (www.unaids.org). Anti-retroviral therapy (ART) can control viral replication, thereby prolonging progression to AIDS, but the therapy cannot cure HIV infection. There is as yet

[‡]Corresponding Author: Dr. Marjorie Robert-Guroff, Vaccine Branch, CCR, NCI, NIH., 41 Medlars Drive, Building 41, Room D804, Bethesda, MD 20892-5065, Phone: (301) 496-2114; Fax: (301) 402-0055; guroffm@mail.nih.gov.

[1]This study was supported by the Intramural Research Program of the NIH, National Cancer Institute.

no highly effective vaccine against HIV infection. Until recently HIV vaccine development was focused on induction of cellular immunity. However, after the modest success of the RV-144 phase III clinical trial which confirmed the importance of humoral immunity for HIV protective efficacy (1), the focus has shifted to development of vaccines that can induce B cell maturation and elicit Env-specific antibodies, memory B cells and long lived plasma cells.

Multiple important roles are played by B cells during the induction of immune responses to vaccines. They can act as antigen presenting cells and also as effector cells, producing antibodies, cytokines, adhesion molecules and chemokines (2–4). They have been reported to exert immune suppressive effects (5, 6) and to regulate T cell immunity in chronic hepatitis B infection and to impair CTL activity during HIV infection (7, 8). Both HIV and SIV infections lead to severe B-cell dysregulation and dysfunction in their respective hosts (9, 10).

The B cell dysfunction caused by HIV cannot be completely reversed by ART treatment (11–13). Therefore, a prophylactic vaccine targeting B cells needs to induce potent, broad humoral immunity that confers sterilizing protection or alternatively a response sufficient to clear infectious viral foci prior to systemic dissemination of the virus in order to avoid B cell dysfunction and maintain effective humoral immunity. An in-depth understanding of B cell dynamics and sub-populations will facilitate the development of an efficacious HIV/SIV vaccine.

Many vaccines are tested pre-clinically in rhesus macaques, an established animal model for HIV and SIV vaccine development (14, 15). We have used this model extensively to evaluate candidate vaccines and assess induction of humoral immunity and B cell maturation and development. A sex bias is well known in viral diseases, including HIV/AIDS in which HIV infected women exhibit higher baseline CD4 T-cell counts and lower HIV RNA levels than men (16). However, until our recent pre-clinical macaque study, an HIV/SIV vaccine-related sex bias in protective efficacy had not been described. We reported vaccine-induced delayed SIV_{mac251} acquisition in female but not male rhesus macaques (17). The basis for this sex bias appeared to be vaccine-induced B cell immunity at mucosal sites, including SIV Env-specific IgA antibodies in rectal secretions, rectal Env-specific memory B cells, and total rectal plasma cells (PC).

In the current study we sought to uncover additional parameters associated with the observed sex bias by studying the dynamics of memory B cell populations in three different tissues during immunization and following infection, the role of IgG subtypes in influencing functional immune responses, and antibody avidity. In view of a previous report showing that $CD4^{+}CD25^{high}$ regulatory T cells contribute to a sex difference in the prevalence of autoimmune diseases (18), we investigated whether B_{reg} cells might also contribute to a sex bias in vaccine outcome. We show that in addition to the importance of the previously identified mucosal B cell immunity, factors associated with the observed sex bias in vaccine-induced delayed SIV acquisition include antigen specific IgG3 antibody in females and higher levels of suppressive $CD19^{+}CD25^{high}$ B_{reg} cells in males.

MATERIALS AND METHODS

Animals, immunization and challenge protocols

The Indian rhesus macaques used in this study and the vaccine regimen and challenge protocol have been previously described (17). Briefly, macaques were primed at weeks 0 (intranasally and orally) and 12 (intratracheally) with three replication-competent Adenovirus 5 host range mutant (Ad5hr) recombinants separately encoding SIV_{smH4}*env*(gp140)/*rev*, SIV_{239}*gag* and SIV_{239}*nef*Δ_{1-13}. The boosting immunogens were administered intramuscularly at weeks 39 and 51 in MF59 adjuvant. The gp120 immunization group (16 females and 8 males) received soluble monomeric SIV_{239} gp120, and the gp140 immunization group (16 females and 8 males) received oligomeric SIV_{239} gp140, both made in CHO cells (Novartis). Control macaques (7 females and 5 males) received Ad5hrΔE3 vector and MF59 adjuvant. At week 59, intrarectal repeated weekly low dose challenges of SIV_{mac251} were initiated. Plasma viral loads were determined using the NASBA technique (19). Infection was determined by viral loads ≥50 SIV RNA copies/ml. One female in the gp140 group remained uninfected after 9 challenges. Results on this macaque are included except in analyses involving post-infection time points and viral load.

Sample collection

Blood and bone marrow samples were centrifuged over Ficoll gradients to obtain single cell suspensions (13). After washing and lysis of contaminating red blood cells, PBMCs and bone marrow cells were stored in FBS/10% DMSO in liquid nitrogen until used. Rectal biopsies were rinsed with pre-warmed RPMI1640 (Invitrogen) containing 2×antibiotic–antimycotic solution, 2-mM L-glutamine (Invitrogen) and 2 mg/ml Collagenase (Sigma–Aldrich). Prior to incubation (25 min at 37°C) the pinches were minced using a scalpel and a 19G needle, transferred in 10 ml of the same media to a 50 ml tube and pulse vortexed every 5 min. The digested tissue was passed 5 times through a blunt end cannula. The liberated cells and tissue debris were passed through a 70 μm cell strainer, and the cells were washed in R10 (RPMI1640 containing 2×antibiotic–antimycotic solution, L-glutamine and 10% FBS) prior to staining.

Flow Cytometry

Cells ($1–2\times10^6$/tube) were stained with the antibodies listed in Table 1. After a 25 min surface staining and envelope protein staining (20), cells were washed with 2% FBS in PBS, fixed and permeabilized for 15 min at room temperature using a transcription buffer set for IRF-4 (BD Bioscience, San Jose, CA). After washing in Permwash solution, intracellular staining was conducted. Subsequently, cells were washed and resuspended in PBS and acquired within 2 hours on a custom 4-laser LSR II (BD Bioscience). Samples were diluted in sheath fluid and cells obtained from rectal pinches and bone marrow were passed through a 35 μm cell strainer. A minimum of 50000 live cells in the lymphocytic gate were acquired in DIVA. Analysis was performed in FlowJo, and data were exported into Excel and Graphpad Prism 6. Envelope specific memory B cells were defined as described previously (20), as were plasmablasts (PB) and PC in mucosal tissues (21). The suppressive B_{reg} cells were identified as $CD19^+CD25^{high}$.

Sorting of B_{reg} cells and functional suppression in a T cell proliferation assay

To sort purified macaque $CD19^+CD25^{high}$ B_{reg} cells and $CD3^+CD4^+$ T cells, peripheral blood mononuclear cells (PBMCs) obtained from naïve macaques were surface stained with anti-CD25 (clone BC96, eBioscience), anti-CD3, anti-CD4 and anti-CD19 (Beckman Coulter). The dead cells were gated out using aqua blue dead cell dye (Invitrogen). Sorting was performed using a MoFlo Astrios EQ. Three populations were sorted: $CD19^+CD25^{high}$, $CD19^+CD25^-$ and $CD3^+$ $CD4^+$. The $CD3^+CD4^+$ T cells were labeled with CFSE (Invitrogen) according to the manufacturer's instructions. These labeled T cells were co-cultured either with $CD19^+CD25^{high}$ or $CD19^+CD25^-$ cells at a 1:1 ratio in an anti-CD3 (FN18, from the Nonhuman Primate Reagent Resource, 10 μg/ml) coated U-bottom 96-well plate in the presence of anti-CD28 (CD28.2, NIH Nonhuman Primate Reagent Resource, 1 μg/ml) and IL-2 (100 units/ml; NIH Resource for Nonhuman Primate Immune Reagents). The cells were cultured at 37°C for 72 hours. As controls, unlabeled and CFSE-labeled $CD4^+$ T cells were cultured with or without any of the stimuli. Analysis of the CFSE pattern of $CD4^+$ T cells in the different conditions was performed using FlowJo analysis software (Tree Star, Ashland, OR, USA). The proliferating cells were expressed as the percentage of $CFSE^+$ $CD4^+$ T cells excluding generation 0.

IL-10 gene expression in $CD19^+CD25^{high}$ B_{reg} cells

Total RNA was isolated from $CD19^+CD25^{high}$ and $CD19^+CD25^-$ B cells using RNeasy Mini Kits (Qiagen) as described by the manufacturer's protocol. For mRNA analysis, the total RNA was reverse transcribed using a QuantiTect Reverse Transcription Kit (Qiagen). Specific primers for IL-10 and 18S from Eurofins MWG Operon (Huntsville, AL, USA) were used to amplify cDNA. Samples were run in a 25 μl reaction using KAPA SYBR FAST premix with ROX Low (KAPA Biosystems) on an Applied Biosytems ABI7500 cycler (Life Technologies) under the following conditions: 10 min 95°C and 40 cycles of 30s 95°C, 15s 59°C and 30s 72.5°C followed by standard melting curve analysis. The primers for QRT-PCR were: IL-10 forward (F) 5′ AGAACCACGACCCAGACATC 3′, IL-10 reverse (R) 5′ GGCCTTGCTCTTGTTTTCAC 3′; 18S F 5′ GCCCGAAGCGTTTACTTTGA 3′, 18S R 5′ TCCATTATTCCTAGCTGCGGTATC 3′ (22, 23). Gene expression levels were normalized against 18S RNA as reference gene. The comparative C_T method ($\Delta\Delta C_T$ method) was used to determine the quantity of the target sequences. Relative expression levels were presented as the relative fold change and calculated using the formula: $2^{-\Delta\Delta CT}$

IgG subclass antibody binding titer

Half area plates were coated either with 50 μl of 1μg/ml of SIV_{mac239} gp140 or gp120 in carbonate-bicarbonate buffer (pH 9.6) overnight at 4°C. The plates were blocked with 100 μl of 1% BSA in D-PBS for 1 h at 37°C. Serum samples were diluted 1:100 for IgG2, 1:200 for IgG3 and 1:2000 for IgG1 in D-PBS containing 1% BSA and 0.05% Tween20. 50 μl of serial two-fold dilutions of sera were incubated on the plate for 1 h at 37°C. Primary antibodies including unlabeled IgG2 at 1:1000, IgG3 at 1:2000 dilution, and HRP conjugated IgG1 at 1:5000 were obtained from the NIH Nonhuman Primate Reagent Resource. Jackson goat anti-mouse HRP was used as the detection antibody at a 1:10000 dilution for IgG2 and IgG3. 3,3′,5,5′-tetramethylbenzidine (TMB) substrate development

was done for 20 min at room temperature before stopping the reaction with 1 M phosphoric acid. Plates were read at 450 nm. The antibody titer was defined as the serum dilution at which the absorbance of the test serum was twice the mean absorbance of 12 blank wells. Subclass antibody titers were subsequently expressed as the percentage of the pan IgG antibody titer. The latter titers were determined as reported previously (13, 17).

Serum binding antibody avidity

The avidities of Env-specific IgG and IgG3 antibodies were evaluated by parallel ELISA as previously described (24, 25). Briefly, half area plates were coated with 50 μl of 1μg/ml SIV_{mac239} gp140 or gp120 in carbonate-bicarbonate buffer (pH 9.6) overnight at 4°C. The plates were blocked with 100 μl of 1% BSA in D-PBS for 1 h at 37°C. Serum samples were diluted 1:100 for IgG3 and 1:1000 for IgG in D-PBS containing 1% BSA and 0.05% Tween20. 50 μl of serial two-fold dilutions of sera were incubated on the plate for 1 h at 37°C. The plate was then washed and half the samples were treated with 100 μl of PBS while the paired samples were treated with 1.5 M sodium thiocyanate (NaSCN; Sigma-Aldrich) for 10 min at room temperature. HRP-conjugated goat anti-monkey IgG (AlphaDiagnostic) and TMB substrate (KPL) were used in sequential steps, followed by reading the OD at 450 nm. For IgG3 a primary antibody obtained from the Nonhuman Primate Reagent Resource was used at a dilution of 1:2000 and Jackson goat anti-mouse HRP was used as the detection antibody at a 1:10000 dilution. Titers of the NaSCN- and PBS-treated sera were defined as the reciprocal of the serum dilution giving an OD twice the OD of a negative macaque serum. The avidity index was then calculated as the ratio of the NaSCN-treated serum titer to the PBS-treated serum titer multiplied by 100. Pre immunization sera served as negative controls.

Non-neutralizing antibody activities

Serum antibody-dependent cell-mediated cytotoxicity (ADCC) was evaluated using a rapid fluorometric assay as previously described (26). ADCC endpoint titers are defined as the reciprocal dilution at which the percent ADCC killing was greater than the mean percent killing of the negative controls plus three standard deviations.

Antibody-dependent cellular phagocytosis (ADCP) activity was measured as previously described (27), with minor modifications (17). The phagocytic score of each sample was calculated as follows: (% phagocytosis × MFI)/$10^{6.}$ The values were standardized to background values (cells and beads only without serum) by dividing the phagocytic score of the test sample by the phagocytic score of the background sample.

Statistical analysis

Data were analyzed using Prism (v6.0, GraphPad Software). A p value ≤ 0.05 was considered statistically significant. The Wilcoxon signed rank test was used to analyze paired data, the Mann-Whitney test was used to analyze unpaired data, and the Spearman rank correlation test was used to assess immunological correlates. Adjustments for multiple comparisons were not made.

RESULTS

SIV_{mac251} Envelope specific memory B cell induction in different tissues following immunization and analysis by sex

To assess the B cell response to the vaccine regimen we initially examined the dynamics of B cell memory development over the course of immunization and following infection by quantifying SIV_{mac251} Env-specific memory B cells in different tissues (20). The tissue samples examined included: PBMC, bone marrow and rectal biopsies. Env-specific memory B cells were induced significantly in PBMC during immunization, increasing steadily following the Ad5hr-recombinant priming immunizations and the two Env boosts (Fig. 1A), however the level dropped slightly post-infection (Fig. 1A). Env-specific memory B cells appeared in bone marrow after the Ad5hr-recombinant primes, but dropped slightly following Env boosting (Fig. 1B). The level significantly increased after infection, reflecting increased antigen exposure (Fig. 1B). Env- specific memory B cells in rectal biopsies were not quantified prior to immunization or following Ad5hr-recombinant priming due to lack of samples. However, comparisons with control unimmunized macaques tested at the same time points showed significant induction of Env-specific memory B cells following the second Env boost and again post-infection, reflecting the increased viral loads at the mucosal site of infection (Fig. 1C). By 8 weeks post-infection (wpi), the level of Env-specific memory B cells in rectal tissue had begun to wane. Overall, the vaccination protocol induced significant SIV Env-specific memory B cells both systemically and mucosally.

In our previous study, delayed SIV acquisition was seen in female but not male vaccinated macaques (17). Therefore, we analyzed Env-specific memory B cells in the three tissues by sex. In PBMC, elevated Env-specific memory B cells were seen in males compared to females 2 wpi (Fig. 1D). No sex difference was observed in the bone marrow (Fig. 1E), whereas as previously reported (17) Env-specific memory B cells in rectal tissue were higher in females than males 2 wpi suggesting better anamnestic responses at the site of infection.

Because in the previous study delayed SIV acquisition in female macaques was more pronounced in those vaccinated with gp120 rather than gp140 (17) we also analyzed the memory B cell data by immunization group. Over the course of immunization and following infection, no differences in Env-specific memory B cell levels between gp120- and gp140-immunized macaques were seen at any time point in any of the three tissues (Suppl Fig. 1 A–C).

Total plasmablasts and plasma cells

PB and PC are the antibody secreting cells which ultimately provide long-lasting humoral immunity. We previously assayed these cell populations in bone marrow using the ELISPOT technique. Both IgG and IgA Env-specific PB/PC were elicited by the immunization regimen and displayed anamnestic responses 2 wpi, significantly elevated above pre-challenge levels (17). PB/PC responses tended to be higher in the gp140 immunization group, however no sex differences in either IgG or IgA PB/PC levels were observed (17). As sufficient rectal cells were not available for Env-specific ELISPOT assays, we used flow cytometry to examine total PB and PC populations. Mucosal PB were identified as

$CD19^+CD20^{+/-}HLA\text{-}DR^+Ki\text{-}67^+IRF4^+CD138^{+/-}$ and PC as $CD19^+CD20^-HLA^-DR^-Ki\text{-}67^-IRF4^+CD138^+$ as previously described (21).

Total rectal PB levels in the interval between the second Env boost and 2 wpi significantly declined with a subsequent slight rebound 8 wpi (Fig. 2A). In contrast total PC remained relatively constant in the interval between immunization and 2 wpi, but increased dramatically 8 wpi (Fig. 2B) suggesting homing of PC to the mucosal tissue or perhaps maturation of PB in response to the increased viral load. We previously reported that mucosal PC of vaccinated females two wpi were significantly correlated with delayed viral acquisition (17). Here, no sex differences in PB or PC levels in rectal tissue were observed (Fig. 2C, D) although PC levels in females 2wpi tended to be elevated compared to the males. Further, no differences in PB/PC responses were observed in rectal tissue with respect to immunization group (Suppl. Fig 1 D, E.)

Overall, while systemic B cell responses did not elucidate any factors associated with the observed delayed acquisition, the rectal tissue data highlighted the potential role of mucosal B cells in the challenge outcome.

Immunological correlates of IgG subclasses in female macaques

Although as reported earlier vaccinated females exhibited delayed SIV acquisition, the vaccinated male macaques exhibited higher serum antibody binding titers (17). Therefore, we considered that the quality of the systemic antibody response may have differed between the sexes. IgG is one of the most abundant antibodies in human serum and is divided into four subclasses: IgG1, IgG2, IgG3, and IgG4 (28). IgG1 is primarily induced by soluble protein antigens and membrane proteins, but its induction is accompanied by lower levels of the other subclasses, mostly IgG3 (29). Vaccine induction of antigen specific IgG3 is of particular interest because IgG3 antibodies are potent pro-inflammatory antibodies and interact strongly with Fc receptors, thereby effectively mediating antibody-dependent effector functions. IgG3 also binds C1q in the classic pathway of complement activation with the highest affinity (30). Importantly in the RV144 clinical trial, HIV-specific IgG3 antibodies were correlated with decreased risk of HIV infection (31).

Here we measured end point binding titers specific for SIV_{mac239} gp120 and gp140 for three subclasses of IgG, namely IgG1, IgG2, and IgG3 in sera 2 weeks after the 2^{nd} Env boost. Reagents for evaluating IgG4 in macaques were not available. To take into account the greater abundance of IgG1 in the serum samples tested which might have competed with the other antibody subtypes, we report the results here as percent of pan IgG responses as outlined in Materials and Methods. Vaccinated female macaques exhibited significantly higher levels of IgG3 gp120-specific antibody compared to males, with IgG1 and IgG2 levels approaching a significant difference (Fig. 3A). Similarly, females in the gp140-immunization group exhibited higher levels of all three subclasses (IgG1, IgG2 and IgG3) compared to males (Fig. 3B). There was no difference between immunization groups in levels of Env specific IgG1, IgG2, or IgG3 (Suppl. Fig. 2).

To determine the relative contribution of the Env-specific antibodies of differing subclasses in males and females to non-neutralizing antibody activities, we conducted correlation

analyses. The % gp140-specific IgG3 of all immunized females but not males significantly correlated with the ADCC titer against gp120 targets (Fig. 4A, B). Moreover, the % gp140-specific IgG3 values of females significantly correlated with antibody-dependent phagocytosis activity (Fig. 4 C) whereas those of males did not, perhaps due to the small sample size (Fig. 4D). To determine if these effector functions impacted viremia control, we conducted correlations with viral loads. The % gp140-specific IgG3 in females but not males exhibited a significant negative correlation with peak viral load (Fig. 4E, F). Taken together, these correlations suggested that in spite of overall higher antibody binding titers in immunized males, the immunized females generated higher quality antibodies able to better mediate effector functions.

Immunized males exhibit higher antibody avidity

To further characterize the vaccine-induced antibodies, we determined the serum binding avidity index of Env-specific IgG and IgG3 in sera 2 weeks post 2nd boost. Surprisingly, the gp120 specific IgG avidity index in immunized males was marginally significantly higher than the avidity index in immunized females (Fig. 5A). However, this slight elevation in males was not reproduced significantly in avidity values for gp140 specific IgG, or in the gp120 or gp140 specific IgG3 avidity indices (Fig. 5A, B). While no differences by immunization group were seen in the gp120-specific IgG3 avidity indices (Fig. 5C), as expected, the gp140 specific IgG and IgG3 avidity indices of animals immunized with oligomeric gp140 were significantly higher compared to animals immunized with monomeric gp120 (Fig. 5D). Overall, avidity differences did not explain the observed sex bias in vaccine outcome.

$CD19^{+}CD25^{high}$ B_{reg} cells in males

B-cells have a complex role in the immune response. A recently characterized B_{reg} cell subset, expresses CD20 and CD25 and exhibits immunoregulatory properties (32). Some studies have reported that $CD25^{+}$ B cells display a better antigen-presenting cell capacity and secrete significantly higher levels of the immunosuppressive cytokine, IL-10, than $CD25^{-}$ B cells (5, 32–34). In a human study $CD19^{+}$ $CD25^{high}$ B_{Regs} were shown to suppress $CD4^{+}$ T cell proliferation (5). As regulatory T cells have been shown to mediate a sex difference in autoimmune diseases (18), we questioned whether the sex bias associated with B cell immunity that we reported previously (17) may have been related to differences in B_{reg} cells. Therefore, we quantified cells with a $CD19^{+}CD25^{high}$ phenotype in PBMCs obtained from all the immunized animals 3 days after the second Env boost by flow cytometry and analyzed the results by immunization group and sex. We did not find any significant difference in the proportion of B_{reg} cells between immunization groups. However, we saw a significantly higher frequency of $CD19^{+}CD25^{high}$ B cells in males, following the Env boost and 8 wpi (Fig. 6A). Moreover, the levels of $CD19^{+}CD25^{high}$ B cells following immunization positively correlated with peak viral loads in males ($p=0.0071$, Fig. 6B) but not in females, suggesting that the presence of high levels of suppressive B cells in males could have had an adverse effect on the challenge outcome. The 3 day post-second boost PBMCs were the only samples available for B_{reg} analysis, as samples collected at other time points had been used in other experiments. Whether this time point was optimal remains to be determined in future studies.

In humans, B_{reg} cells have been phenotyped using CD24, IL-10, and Fox-P3 markers (35) (6, 34). As we were not able to identify reliable antibody clones that recognized CD24 in macaques we identified B_{reg} cells as $CD19^{+}CD25^{high}$ as previously described (5, 6). To substantiate the suppressive function of these cells, we co-cultured CFSE labeled anti-CD3/CD28 activated $CD3^{+}CD4^{+}$ T cells either with $CD19^{+}CD25^{high}$ or $CD19^{+}CD25^{-}$ B cells. T cell proliferation was suppressed when co-cultured with $CD19^{+}CD25^{high}$ B cells but was not affected when co-cultured with $CD19^{+}CD25^{-}$ B cells ($p=0.031$, Fig. 7A). Moreover, the $CD19^{+}CD25^{high}$ B cells exhibited significantly higher levels of IL-10 gene expression compared to $CD19^{+}CD25^{-}$ B cells ($p=0.031$, Fig. 7B).

DISCUSSION

We previously reported a vaccine-induced delay in SIV acquisition in female but not male macaques that correlated with local mucosal antibody responses and elevated memory B cell and PC frequencies at the site of exposure (17). To elucidate additional factors associated with this vaccine outcome, we investigated memory B cell subpopulations in both systemic and mucosal compartments: peripheral blood, bone marrow, and rectal tissue. We reasoned that observed frequencies of B cell memory subpopulations would suggest trafficking patterns associated with the vaccine regimen and subsequent rectal SIV challenge. Env-specific memory B cells were induced significantly post-immunization and/or post-infection in all three tissues (Fig. 1A–C). In PBMC the cells increased steadily over the course of immunization, with a slight decrease occurring 2 wpi (Fig. 1A). In contrast, in BM, a similar increase in frequency did not result from the booster immunization. Notably, however, Env-specific memory B cells exhibited a sharp increase in frequency 2 wpi in both BM and rectal tissue (Fig. 1B,C), the latter most likely resulting from exposure to the viral Env antigen. Examination of differences between males and females indicated that male macaques developed higher Env-specific memory B cell levels in peripheral blood post-infection. In contrast, females exhibited a higher frequency of Env-specific memory B cells in the rectal mucosa 2 wpi (Fig.1F) as previously reported (17). Other than our previous observations of Env-specific mucosal IgA, rectal Env-specific memory B cells, and rectal PC associated with delayed acquisition (17), our study here of B cell dynamics across the three tissues did not reveal any additional immune correlates. However, SIV infection can induce severe B cell dysfunction and dysregulation, with loss of both naïve and memory B cells occurring during acute infection (10). The dynamics of PB and PC throughout the vaccine regimen and post infection in bone marrow and rectal tissue were therefore of interest with regard to potential maintenance of B cell memory. We previously reported that PB/PC levels in BM evaluated by ELISPOT increased in the interval between the last immunization and 2 wpi (17). Here we observed that while Env-specific memory B cells decreased in PBMC 2 wpi, in rectal tissue the PB level decreased at the same time while the PC level was relatively constant during the same interval, and had increased significantly by 8 wpi (Fig. 2). It is not clear whether these B cell subpopulations trafficked to the rectal mucosa as a result of viral exposure. The increase in rectal PC suggests that the vaccine was able to prevent early B cell dysfunction by recruiting, maintaining, and/or inducing PC at the site of infection up to 8 wpi. Studying B cell dynamics in samples from the chronic phase of infection should elucidate the duration of this vaccine effect. Until a method to quantify Env-specific PC

becomes available, it will be difficult to confirm this argument and track the movement of these B cells between various tissue compartments.

One of the conundrums in our previous study was that the male macaques exhibited higher Env-specific binding antibodies than the females, yet the females exhibited better protection, which was associated with humoral responses (17). To address this, we tested the hypothesis that the females generated better quality antibodies. We first analyzed levels of IgG subclasses and antibody avidities in sera obtained following the 2nd boost. Females exhibited significantly higher levels of gp120-specific IgG3 and gp140-specific IgG1, IgG2, and IgG3 antibodies (Fig. 3). However, females did not exhibit higher antibody avidity compared to males (Fig. 5). Nevertheless, significant correlations of non-neutralizing antibody activities with levels of Env specific IgG3 antibody in females but not males strongly supported a difference in antibody quality between the sexes (Fig. 4 A–D). This was further supported by a significant negative correlation of the percentage of Env-specific IgG3 with peak viremia only in female macaques (Fig. 4 E, F). The fact that these significant correlations were obtained with gp140-specific IgG3 antibody levels is consistent with the higher avidity of gp140-specific IgG3 seen in the gp140 immunization group compared to the gp120-immunization group (Fig. 5D). IgG subclasses have varying affinity for Fc receptors which in turn affects their ability to mediate effector functions (36). IgG3 is currently of special interest as V1–V2 antibodies of the IgG3 subclass were correlated with decreased risk of HIV infection in the RV144 trial (31). Further as pointed out by Yates et al., (31) the control of other pathogens has been associated with IgG3 antibodies. Therefore, the correlations seen here in females between Env-specific IgG3 and non-neutralizing effector functions suggest a mechanism underlying the better control of HIV/SIV acquisition. The basis of the better quality IgG3 providing enhanced function in females could include differences in Fc glycosylation, Fc polymorphisms, or recognition of different epitopes, all areas for further investigation.

B cells play many vital roles in vaccine-induced immune response. They also have regulatory functions. B cells that have been identified as regulatory have shown a diversity of phenotypes in mice and humans (37). Here, we characterized B_{reg} cells as $CD19^{+}CD25^{high}$, a subpopulation which has not previously been characterized in rhesus macaques, but one which has been shown to have regulatory function in humans (5, 6). To confirm our identification of macaque B_{reg} cells, we demonstrated that they suppressed T cell proliferation when co-cultured with autologous $CD4^{+}$ T cells and that they exhibited high levels of IL-10 gene expression.

Quantification of $CD19^{+}CD25^{high}$ B cells in circulation after the 2nd Env boost showed that immunized males had significantly higher frequencies of B_{regs} compared to immunized females; moreover, the levels of B_{regs} in immunized males significantly correlated with peak viral loads. The association of B_{reg} cells with viremia was not unexpected in view of earlier reports that activated B cells can produce suppressive cytokines such as IL-10 in response to infectious microorganisms, leading to inhibition of immune functions (38). In fact induction of IL-10-producing B cells was reported to occur early in HIV infection, resulting in suppression of HIV-specific T cell responses (35). Our results showing a positive correlation of macaque $CD19^{+}CD25^{+}$ B_{regs} with peak viremia is consistent with that report which

showed a direct correlation of IL-10^+ B cells with viral loads. Moreover, Siewe et al. (7) reported that in HIV-infected individuals, B_{regs} suppressed $CD8^+$ T cell proliferation, providing a mechanism for lack of viremia control. These observations suggest that in the male macaques, B_{reg} suppressive function resulted in a lesser ability to control early infectious foci, leading to disseminated SIV infection and no apparent delay in acquisition.

The difference in B_{reg} frequencies between male and female macaques was, however, unexpected. To our knowledge, sex differences in B_{reg} cell frequencies have not been reported. It is clear that B_{regs} play an important role in females by insuring tolerance to the fetus during pregnancy (39). B_{regs} have been shown to expand and produce IL-10 in response to estradiol, progesterone, and human chorionic gonadotropin (40). However, the basis for enhanced frequencies of B_{regs} in the male macaques seen here is not known. It is possible that the observation results from looking at a specific subpopulation of B_{regs} and that examining a more comprehensive group of IL-10-producing B cells would provide a different result. Nevertheless, the significant correlation of B_{regs} with peak viremia is consistent with results seen in HIV-infected individuals and together with a possible contribution to the vaccine-induced sex bias provides an important area for further research.

In addition to factors previously identified as correlated with vaccine-induced delayed SIV acquisition in female macaques, including mucosal IgA antibody and enhanced rectal memory B cell subpopulations (17), here we highlight the importance of the IgG3 antibody subclass and the potential impact of B regulatory cells. The vaccine-induced sex bias we have observed is complex and other contributing factors are likely involved. Overall it is a critical area of research that needs both confirmation and further exploration, not only with regard to HIV/SIV prophylactic vaccines, but also for vaccines in general.

Supplementary Material

Refer to Web version on PubMed Central for supplementary material.

Acknowledgments

The following reagents were obtained from the NIH Nonhuman Primate Reagent Resource, Mass Biologics, University of Massachusetts Medical School: anti-CD3, anti-CD4 (OKT4 and T4/19Thy5D7), anti-CD28, anti-IgG2, anti-IgG3, and HRP-conjugated anti-IgG1. IL-2 was obtained from the NIH Resource for Nonhuman Primate Immune Reagents, Emory University.

References

1. Rerks-Ngarm S, Pitisuttithum P, Nitayaphan S, Kaewkungwal J, Chiu J, Paris R, Premsri N, Namwat C, de Souza M, Adams E, Benenson M, Gurunathan S, Tartaglia J, McNeil JG, Francis DP, Stablein D, Birx DL, Chunsuttiwat S, Khamboonruang C, Thongcharoen P, Robb ML, Michael NL, Kunasol P, Kim JH, MT Investigators. Vaccination with ALVAC and AIDSVAX to prevent HIV-1 infection in Thailand. N Engl J Med. 2009; 361:2209–2220. [PubMed: 19843557]
2. Porakishvili N, Mageed R, Jamin C, Pers JO, Kulikova N, Renaudineau Y, Lydyard PM, Youinou P. Recent progress in the understanding of B-cell functions in autoimmunity. Scand J Immunol. 2001; 54:30–38. [PubMed: 11439145]
3. Silverman GJ, Carson DA. Roles of B cells in rheumatoid arthritis. Arthritis Res Ther. 2003; 5(Suppl 4):S1–6. [PubMed: 15180890]

4. Anderton SM, Fillatreau S. Activated B cells in autoimmune diseases: the case for a regulatory role. Nat Clin Pract Rheumatol. 2008; 4:657–666. [PubMed: 19037227]
5. Kessel A, Haj T, Peri R, Snir A, Melamed D, Sabo E, Toubi E. Human CD19(+)CD25(high) B regulatory cells suppress proliferation of CD4(+) T cells and enhance Foxp3 and CTLA-4 expression in T-regulatory cells. Autoimmun Rev. 2012; 11:670–677. [PubMed: 22155204]
6. de Andres C, Tejera-Alhambra M, Alonso B, Valor L, Teijeiro R, Ramos-Medina R, Mateos D, Faure F, Sanchez-Ramon S. New regulatory CD19(+)CD25(+) B-cell subset in clinically isolated syndrome and multiple sclerosis relapse. Changes after glucocorticoids. J Neuroimmunol. 2014; 270:37–44. [PubMed: 24662004]
7. Siewe B, Wallace J, Rygielski S, Stapleton JT, Martin J, Deeks SG, Landay A. Regulatory B cells inhibit cytotoxic T lymphocyte (CTL) activity and elimination of infected CD4 T cells after in vitro reactivation of HIV latent reservoirs. PLoS One. 2014; 9:e92934. [PubMed: 24739950]
8. Das A, Ellis G, Pallant C, Lopes AR, Khanna P, Peppa D, Chen A, Blair P, Dusheiko G, Gill U, Kennedy PT, Brunetto M, Lampertico P, Mauri C, Maini MK. IL-10-producing regulatory B cells in the pathogenesis of chronic hepatitis B virus infection. J Immunol. 2012; 189:3925–3935. [PubMed: 22972930]
9. Moir S, Fauci AS. Insights into B cells and HIV-specific B-cell responses in HIV-infected individuals. Immunol Rev. 2013; 254:207–224. [PubMed: 23772622]
10. Kuhrt D, Faith SA, Leone A, Rohankedkar M, Sodora DL, Picker LJ, Cole KS. Evidence of early B-cell dysregulation in simian immunodeficiency virus infection: rapid depletion of naive and memory B-cell subsets with delayed reconstitution of the naive B-cell population. J Virol. 2010; 84:2466–2476. [PubMed: 20032183]
11. D'Orsogna LJ, Krueger RG, McKinnon EJ, French MA. Circulating memory B-cell subpopulations are affected differently by HIV infection and antiretroviral therapy. AIDS. 2007; 21:1747–1752. [PubMed: 17690573]
12. Regidor DL, Detels R, Breen EC, Widney DP, Jacobson LP, Palella F, Rinaldo CR, Bream JH, Martinez-Maza O. Effect of highly active antiretroviral therapy on biomarkers of B-lymphocyte activation and inflammation. AIDS. 2011; 25:303–314. [PubMed: 21192231]
13. Demberg T, Brocca-Cofano E, Xiao P, Venzon D, Vargas-Inchaustegui D, Lee EM, Kalisz I, Kalyanaraman VS, Dipasquale J, McKinnon K, Robert-Guroff M. Dynamics of memory B-cell populations in blood, lymph nodes, and bone marrow during antiretroviral therapy and envelope boosting in simian immunodeficiency virus SIVmac251-infected rhesus macaques. J Virol. 2012; 86:12591–12604. [PubMed: 22973034]
14. Morgan C, Marthas M, Miller C, Duerr A, Cheng-Mayer C, Desrosiers R, Flores J, Haigwood N, Hu SL, Johnson RP, Lifson J, Montefiori D, Moore J, Robert-Guroff M, Robinson H, Self S, Corey L. The use of nonhuman primate models in HIV vaccine development. PLoS Med. 2008; 5:e173. [PubMed: 18700814]
15. Fennessey CM, Keele BF. Using nonhuman primates to model HIV transmission. Curr Opin HIV AIDS. 2013; 8:280–287. [PubMed: 23666391]
16. Addo MM, Altfeld M. Sex-based differences in HIV type 1 pathogenesis. J Infect Dis. 2014; 209(Suppl 3):S86–92. [PubMed: 24966195]
17. Tuero I, Mohanram V, Musich T, Miller L, Vargas-Inchaustegui DA, Demberg T, Venzon D, Kalisz I, Kalyanaraman VS, Pal R, Ferrari MG, LaBranche C, Montefiori DC, Rao M, Vaccari M, Franchini G, Barnett SW, Robert-Guroff M. Mucosal B Cells Are Associated with Delayed SIV Acquisition in Vaccinated Female but Not Male Rhesus Macaques Following SIVmac251 Rectal Challenge. PLoS Pathog. 2015; 11:e1005101. [PubMed: 26267144]
18. Afshan G, Afzal N, Qureshi S. CD4+CD25(hi) regulatory T cells in healthy males and females mediate gender difference in the prevalence of autoimmune diseases. Clin Lab. 2012; 58:567–571. [PubMed: 22783590]
19. Lee EM, Chung HK, Livesay J, Suschak J, Finke L, Hudacik L, Galmin L, Bowen B, Markham P, Cristillo A, Pal R. Molecular methods for evaluation of virological status of nonhuman primates challenged with simian immunodeficiency or simian-human immunodeficiency viruses. J Virol Methods. 2010; 163:287–294. [PubMed: 19878696]

20. Mohanram V, Demberg T, Tuero I, Vargas-Inchaustegui D, Pavlakis GN, Felber BK, Robert-Guroff M. Improved flow-based method for HIV/SIV envelope-specific memory B-cell evaluation in rhesus macaques. J Immunol Methods. 2014; 412:78–84. [PubMed: 24953216]
21. Demberg T, Mohanram V, Venzon D, Robert-Guroff M. Phenotypes and distribution of mucosal memory B-cell populations in the SIV/SHIV rhesus macaque model. Clin Immunol. 2014; 153:264–276. [PubMed: 24814239]
22. Demberg T, Ettinger AC, Aladi S, McKinnon K, Kuddo T, Venzon D, Patterson LJ, Phillips TM, Robert-Guroff M. Strong viremia control in vaccinated macaques does not prevent gradual Th17 cell loss from central memory. Vaccine. 2011; 29:6017–6028. [PubMed: 21708207]
23. Demberg T, Brocca-Cofano E, Kuate S, Aladi S, Vargas-Inchaustegui DA, Venzon D, Kalisz I, Kalyanaraman VS, Lee EM, Pal R, DiPasquale J, Ruprecht RM, Montefiori DC, Srivastava I, Barnett SW, Robert-Guroff M. Impact of antibody quality and anamnestic response on viremia control post-challenge in a combined Tat/Env vaccine regimen in rhesus macaques. Virology. 2013; 440:210–221. [PubMed: 23528732]
24. Zhao J, Lai L, Amara RR, Montefiori DC, Villinger F, Chennareddi L, Wyatt LS, Moss B, Robinson HL. Preclinical studies of human immunodeficiency virus/AIDS vaccines: inverse correlation between avidity of anti-Env antibodies and peak postchallenge viremia. J Virol. 2009; 83:4102–4111. [PubMed: 19224993]
25. Xiao P, Zhao J, Patterson LJ, Brocca-Cofano E, Venzon D, Kozlowski PA, Hidajat R, Demberg T, Robert-Guroff M. Multiple vaccine-elicited nonneutralizing antienvelope antibody activities contribute to protective efficacy by reducing both acute and chronic viremia following simian/human immunodeficiency virus SHIV89.6P challenge in rhesus macaques. J Virol. 2010; 84:7161–7173. [PubMed: 20444898]
26. Gomez-Roman VR, Florese RH, Patterson LJ, Peng B, Venzon D, Aldrich K, Robert-Guroff M. A simplified method for the rapid fluorometric assessment of antibody-dependent cell-mediated cytotoxicity. J Immunol Methods. 2006; 308:53–67. [PubMed: 16343526]
27. Ackerman ME, Moldt B, Wyatt RT, Dugast AS, McAndrew E, Tsoukas S, Jost S, Berger CT, Sciaranghella G, Liu Q, Irvine DJ, Burton DR, Alter G. A robust, high-throughput assay to determine the phagocytic activity of clinical antibody samples. J Immunol Methods. 2011; 366:8–19. [PubMed: 21192942]
28. Schur PH. IgG subclasses. A historical perspective. Monogr Allergy. 1988; 23:1–11. [PubMed: 3290655]
29. Ferrante A, Beard LJ, Feldman RG. IgG subclass distribution of antibodies to bacterial and viral antigens. Pediatr Infect Dis J. 1990; 9:S16–24. [PubMed: 2216603]
30. Bindon CI, Hale G, Bruggemann M, Waldmann H. Human monoclonal IgG isotypes differ in complement activating function at the level of C4 as well as C1q. J Exp Med. 1988; 168:127–142. [PubMed: 3260935]
31. Yates NL, Liao HX, Fong Y, deCamp A, Vandergrift NA, Williams WT, Alam SM, Ferrari G, Yang ZY, Seaton KE, Berman PW, Alpert MD, Evans DT, O'Connell RJ, Francis D, Sinangil F, Lee C, Nitayaphan S, Rerks-Ngarm S, Kaewkungwal J, Pitisuttithum P, Tartaglia J, Pinter A, Zolla-Pazner S, Gilbert PB, Nabel GJ, Michael NL, Kim JH, Montefiori DC, Haynes BF, Tomaras GD. Vaccine-induced Env V1–V2 IgG3 correlates with lower HIV-1 infection risk and declines soon after vaccination. Sci Transl Med. 2014; 6:228ra239.
32. Agematsu K. Memory B cells and CD27. Histol Histopathol. 2000; 15:573–576. [PubMed: 10809378]
33. Brisslert M, Bokarewa M, Larsson P, Wing K, Collins LV, Tarkowski A. Phenotypic and functional characterization of human CD25+ B cells. Immunology. 2006; 117:548–557. [PubMed: 16556269]
34. Amu S, Tarkowski A, Dorner T, Bokarewa M, Brisslert M. The human immunomodulatory CD25+ B cell population belongs to the memory B cell pool. Scand J Immunol. 2007; 66:77–86. [PubMed: 17587349]
35. Liu J, Zhan W, Kim CJ, Clayton K, Zhao H, Lee E, Cao JC, Ziegler B, Gregor A, Yue FY, Huibner S, MacParland S, Schwartz J, Song HH, Benko E, Gyenes G, Kovacs C, Kaul R, Ostrowski M. IL-10-producing B cells are induced early in HIV-1 infection and suppress HIV-1-specific T cell responses. PLoS One. 2014; 9:e89236. [PubMed: 24586620]

36. Ravetch JV, Bolland S. IgG Fc receptors. Annu Rev Immunol. 2001; 19:275–290. [PubMed: 11244038]
37. Mauri C, Bosma A. Immune regulatory function of B cells. Annu Rev Immunol. 2012; 30:221–241. [PubMed: 22224776]
38. Shen P, Fillatreau S. Suppressive functions of B cells in infectious diseases. Int Immunol. 2015; 27:513–519. [PubMed: 26066008]
39. Fettke F, Schumacher A, Costa SD, Zenclussen AC. B cells: the old new players in reproductive immunology. Front Immunol. 2014; 5:285. [PubMed: 25002862]
40. Muzzio D, Zygmunt M, Jensen F. The role of pregnancy-associated hormones in the development and function of regulatory B cells. Front Endocrinol (Lausanne). 2014; 5:39. [PubMed: 24744750]

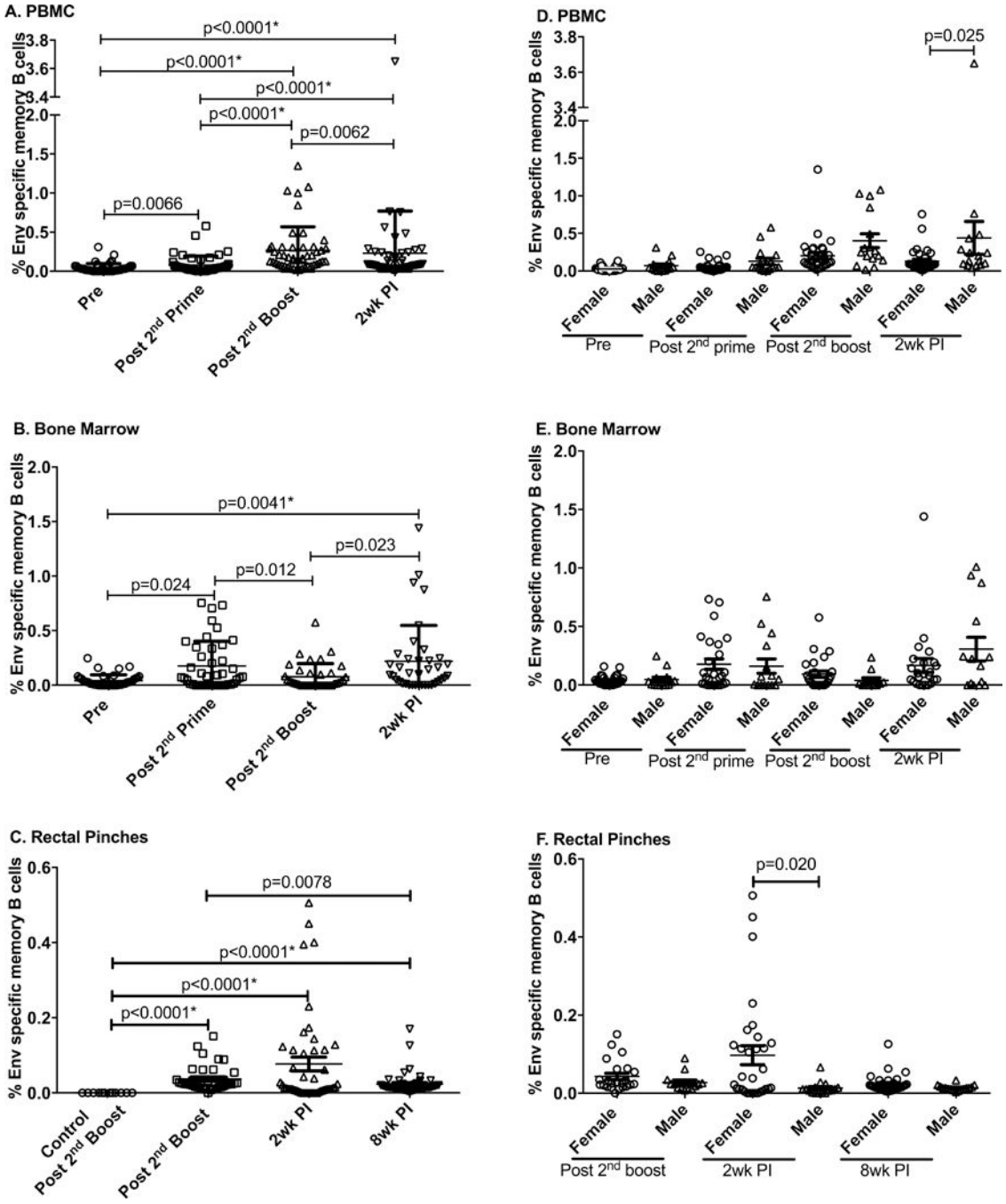

Figure 1. Evaluation of Env-specific memory B cells in vaccinated macaques over the course of immunization and post-SIV$_{mac251}$ infection

PBMC (A), bone marrow (B), and rectal biopsies (C) were obtained from all vaccinated macaques prior to immunization (Pre), 2 weeks after the 2nd Ad immunization (Post-2nd prime), 2 weeks after the 2nd boost (Post-2nd boost) and 2 weeks post-infection (2wk PI) and assayed for Env-specific memory B cells as described in Materials and Methods. As rectal biopsies were not available at the Pre and Post 2nd prime time points, Env-specific memory B cells in vaccinated macaques were compared to levels observed in control macaques that received adjuvant only at the Post-2nd boost time point. Env-specific memory B cells are

shown by sex over the same time course for PBMC (D), bone marrow (E), and rectal biopsies (F). Data presented are means ± SEM. *Remains statistically significant after correction for multiple comparisons.

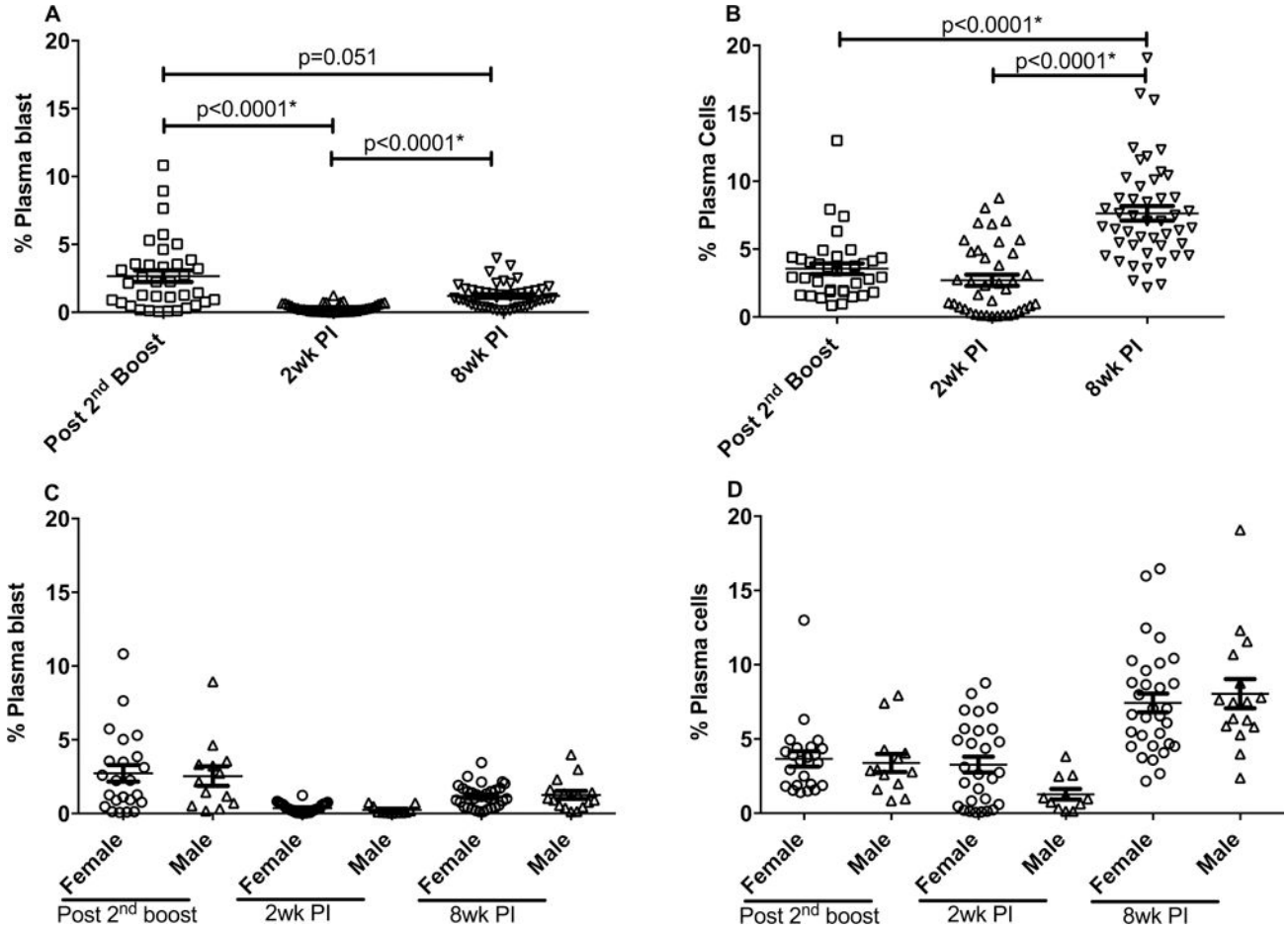

Figure 2. Evaluation of total PB and PC in rectal biopsies in vaccinated and SIV_{mac251}-infected animals

Total PB (A) and PC (B) in rectal biopsies obtained from all vaccinated macaques at the indicated time points (as defined in the legend to Fig. 1) were assayed as described in Materials and Methods. PB and PC analyzed by sex are shown in panels C and D, respectively. The percentages of PB and PC were calculated from the total B cell populations. Data presented are means ± SEM. *Remains statistically significant after correction for multiple comparisons.

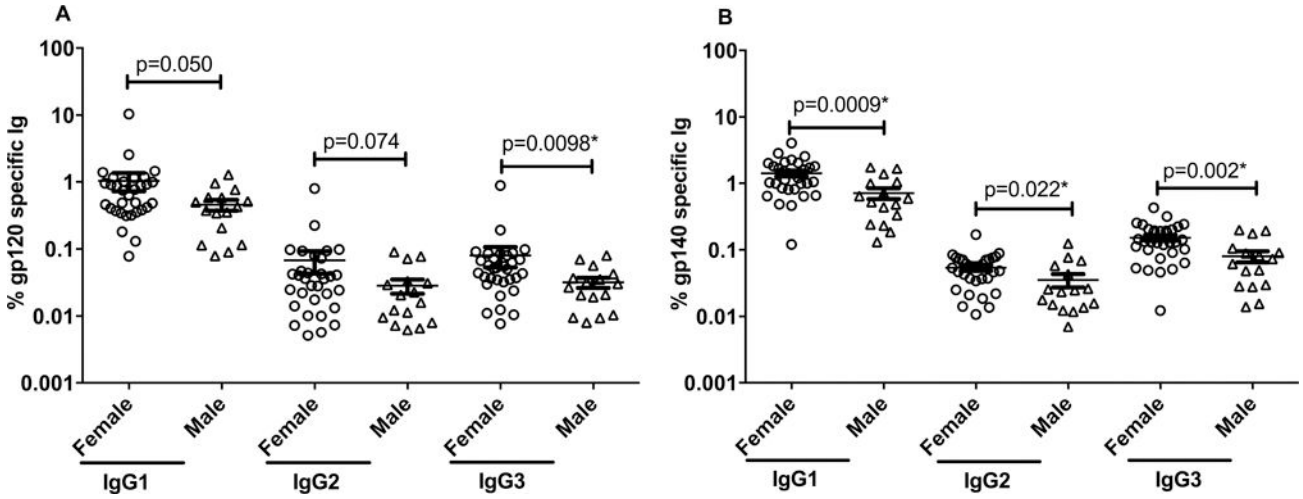

Figure 3. Analysis of Env-specific antibodies of different IgG subclasses, analyzed by sex

gp120- (A) and gp140-specific (B) IgG1, IgG2, and IgG3 antibodies in male and female macaques were assayed on sera obtained 2 weeks after the 2nd boost and expressed as percentages of pan IgG antibody. Data presented are means ± SEM. *Remains statistically significant after correction for multiple comparisons.

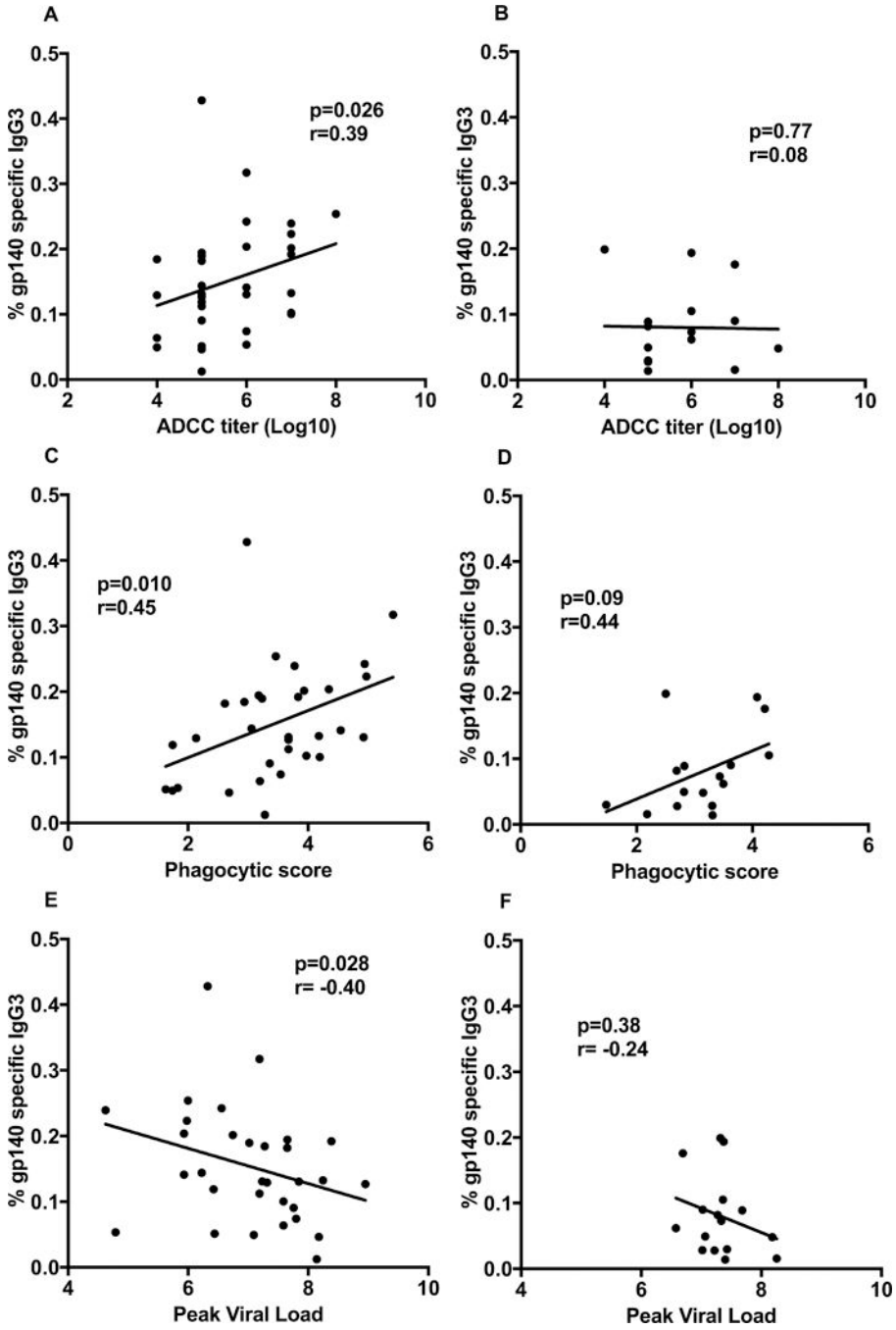

Figure 4. Immunological correlates in females and males

Correlation analyses of data obtained 2 weeks post-2nd boost. Percent of SIV gp140-specific IgG3 with ADCC titer against gp120 targets for (A) all immunized females, and (B) all immunized males. Correlation analysis of percent SIV gp140-specific IgG3 with antibody-mediated phagocytosis for (C) all immunized females, and (D) all immunized males. Correlation analysis of percent SIV gp140-specific IgG3 with peak viral load for all immunized females (E) and all immunized males (F).

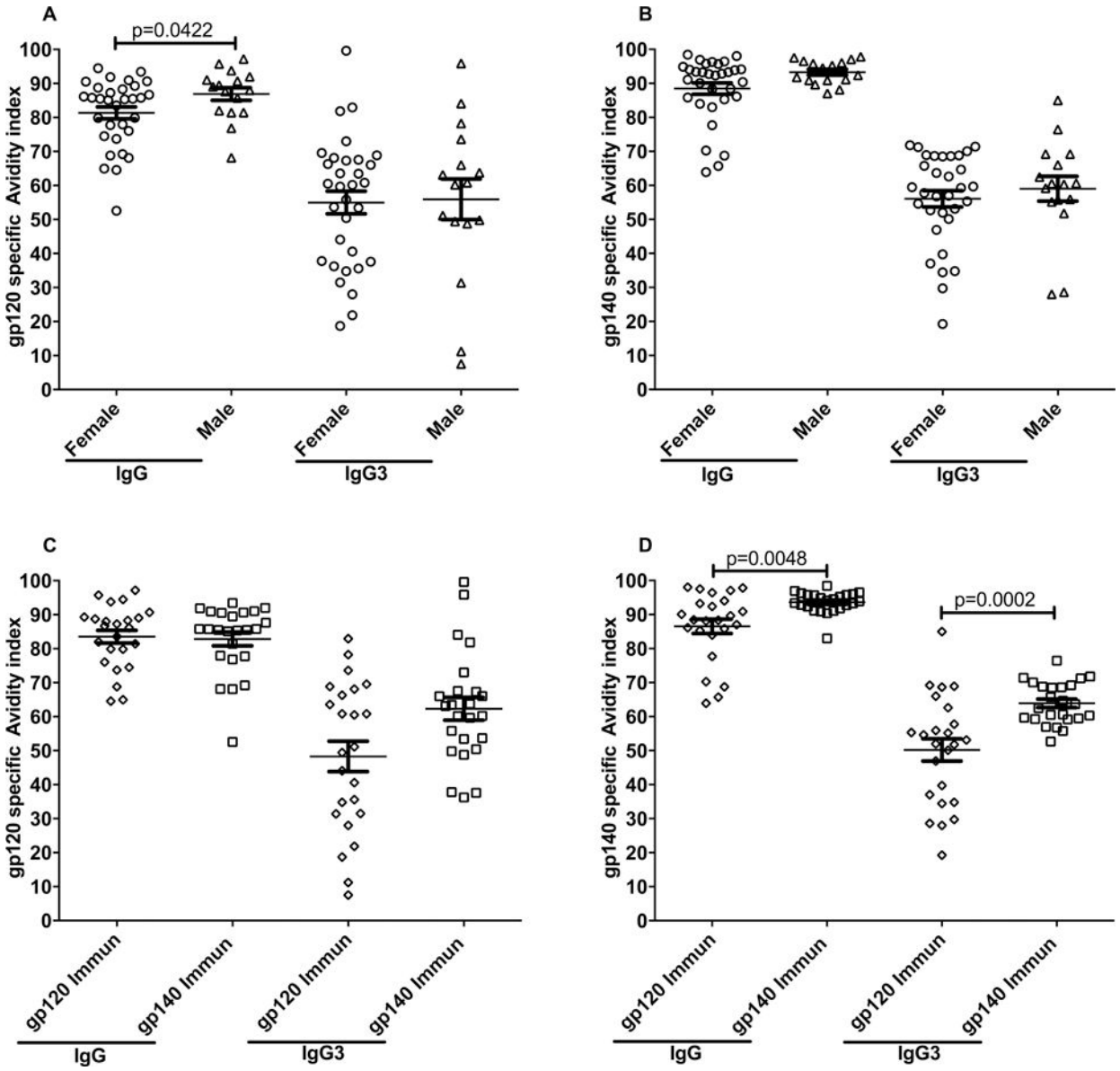

Figure 5. Env-specific IgG and IgG3 avidity indices

IgG and IgG3 antibody avidity indices to SIV_{mac239} gp120 and gp140 were determined on sera obtained 2 weeks post-2nd boost. (A) Male and female SIV_{mac239} gp120-specific avidity indices and SIV_{mac239} gp140-specific avidity indices (B). SIV_{mac239} gp120-specific avidity indices (C) and SIV_{mac239} gp140-specific avidity indices (D) by vaccinated groups. Data presented are means ± SEM.

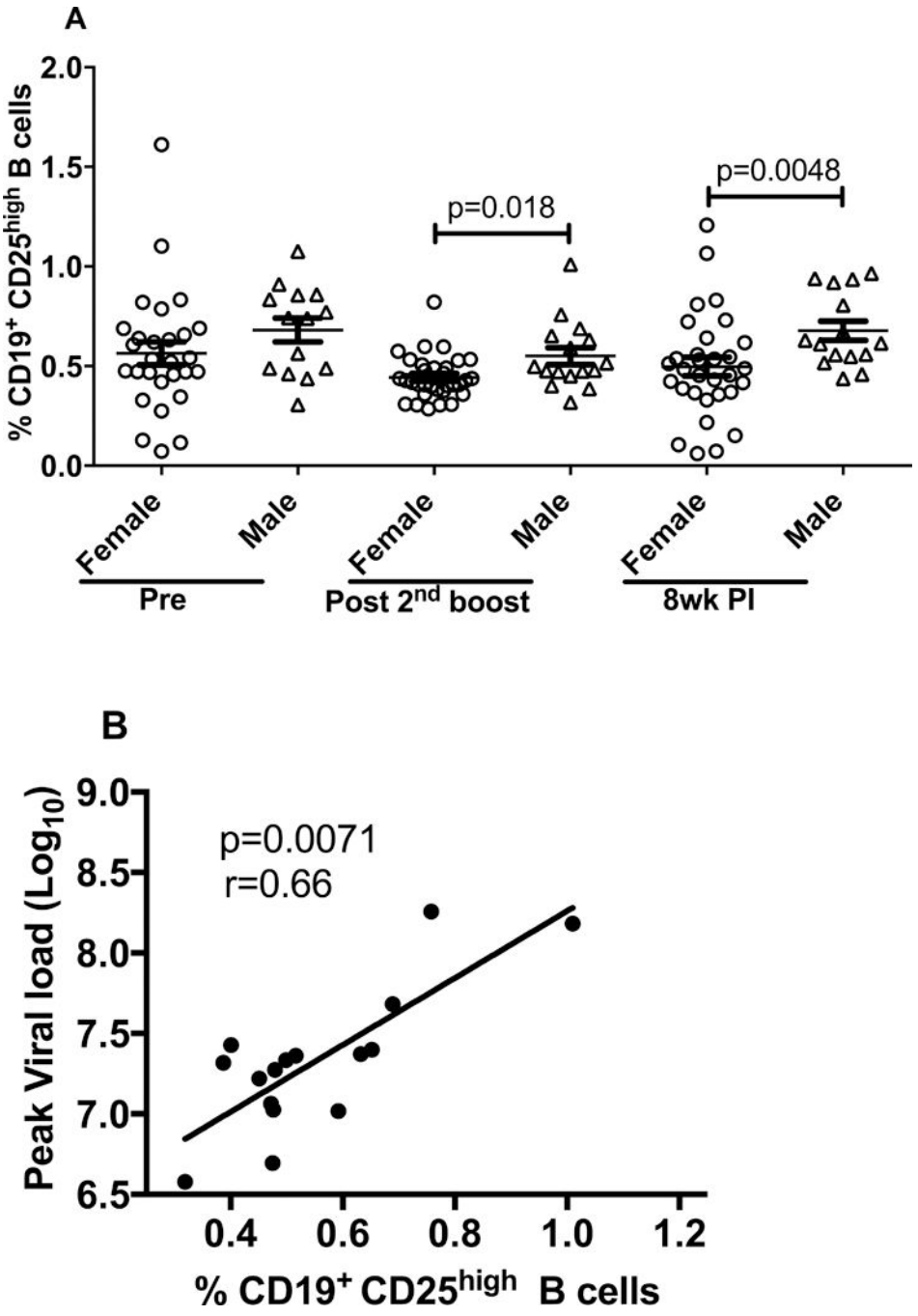

Figure 6. Evaluation and immunological correlates of $CD19^{+}CD25^{high}$ B cells in vaccinated and SIV_{mac251} infected animals

(A) PBMC were obtained at the indicated time points for flow analysis. The post-2nd boost sampling was 3 days following the immunization. (B) Correlation analysis of $CD19^{+}CD25^{high}$ B cells in all immunized males 3 days post-2nd boost with peak viral load. Data presented are means ± SEM.

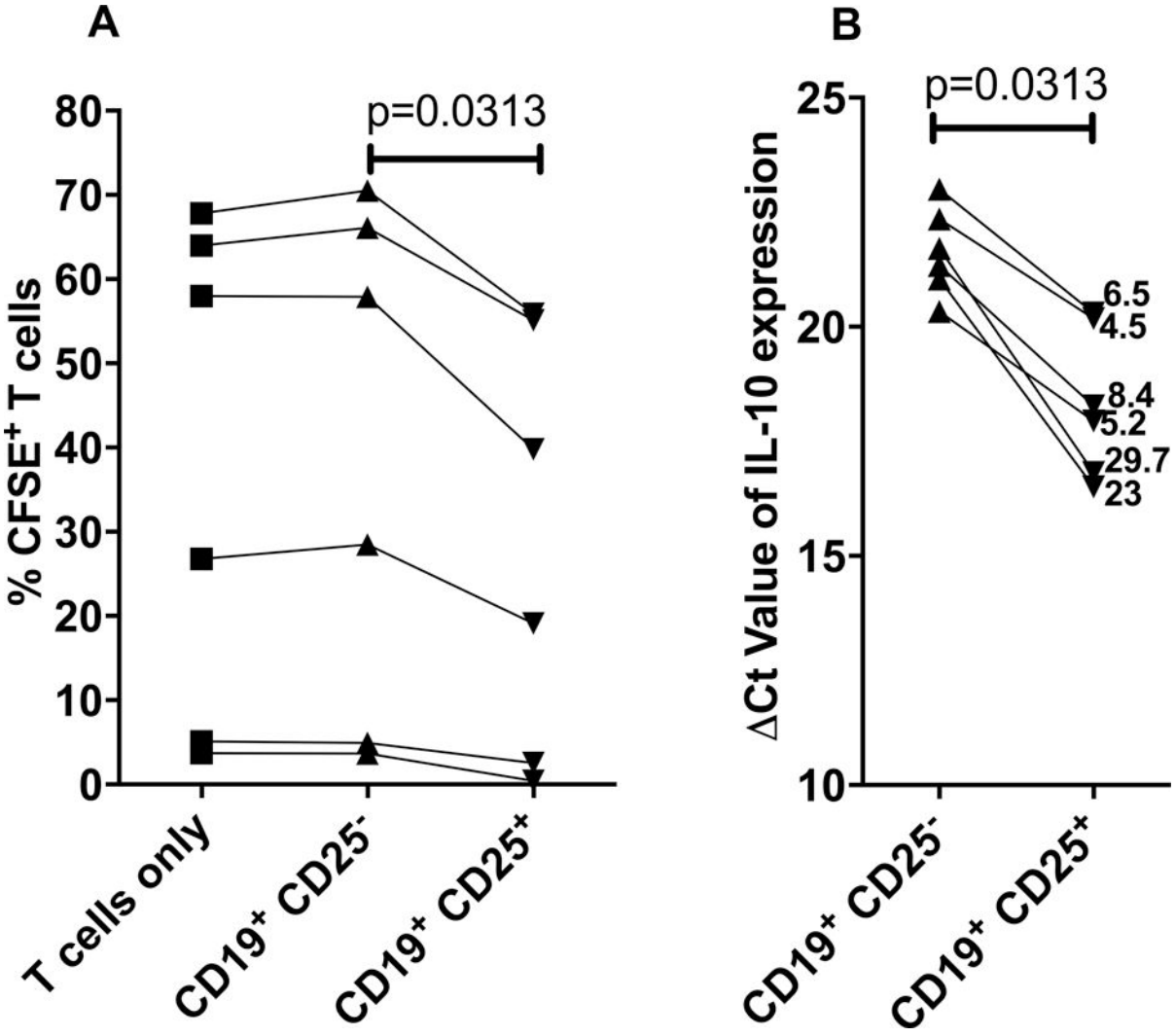

Figure 7. T cell proliferation and IL-10 gene expression

(A) Percentage of CFSE positive T cells excluding generation 0 co-cultured alone or with $CD19^{+}CD25^{high}$ B cells or $CD19^{+}CD25^{-}$ B cells. (B) IL-10 mRNA expression is presented as ΔCt value in $CD19^{+}CD25^{high}$ B cells when compared with $CD19^{+}CD25^{-}$ B cells. The numerical values represent the IL-10 fold increase in $CD19^{+}CD25^{high}$ B cells calculated using the formula $2^{-\Delta\Delta Ct}$.

Table I

Antibodies used for flow cytometry

Antigen	Color	Clone	Host Species	Isotype	Supplier
CD2	Qdot605	S5.5	Mouse	IgG_2a	Invitrogen
CD3	BV605	SP34-2	Mouse	IgG_1,λ	BD Bioscience
CD14	Qdot605/Qdot800	Tu14	Mouse	IgG_2a	Invitrogen
CD19	PE-Cy5	J3-119	Mouse	IgG_1	Beckman Coulter
CD20	eF650NC	2H7	Mouse	IgG_2b,κ	eBioscience
CD21	PE-Cy7	B-ly4	Mouse	IgG_1,κ	BD Bioscience
CD27	PerCP-eF710	O323	Mouse	IgG_1,κ	eBioscience
CD138	PE	DL-101	Mouse	IgG_1,κ	Biolegend
Biotinylated $SIV_{mac251}ENV$	NA	NA	NA	NA	NA
IgD	Texas Red	Polyclonal	Goat	NA	Southern Biotech
IgG	APC-Cy7	G18-145	Mouse	IgG_1,κ	BD Bioscience
Ki-67	A×700	B56	Mouse	IgG_1,κ	BD Bioscience
IRF-4	eFluor660/FITC	3E4	Rat	IgG_1,κ	eBioscience
HLA-DR	Qdot800	Tu36	Mouse	IgG_2b	Invitrogen
CD25	PE-Cy7	BC96	Mouse	IgG_1,κ	eBioscience
CD3	PE	SP34-2	Mouse	IgG_1, λ	BD Bioscience
CD4	APC	L200	Mouse	IgG_1,κ	BD Bioscience
Viability Dye	Aqua	NA	NA	NA	Invitrogen